

A lattice attenuation in Cds measured by the ultrasonic injection method

メタデータ	言語: eng 出版者: 公開日: 2017-10-03 キーワード (Ja): キーワード (En): 作成者: メールアドレス: 所属:
URL	http://hdl.handle.net/2297/24473

A lattice attenuation in CdS measured by the ultrasonic injection method

Tomonobu Hata, Takeshi Nakano, Kikuo Koma, and Toshio Hada

Department of Electrical Engineering, Faculty of Technology, Kanazawa University, 2-40-20, Kodatsuno, Kanazawa, Japan

(Received 3 January 1978; accepted for publication 13 April 1978)

This paper concerns the use of Brillouin scattering measurements to study lattice attenuation in semiconducting CdS crystals. Measured acoustic fluxes are produced by the acoustoelectric domains. In order to measure the attenuation constant, an ultrasonic injection method is applied. A sample is divided into two parts; one part is used as a generation region of the acoustic flux [region (1)] and the other part is used as a propagation region of the injected flux [region (2)]. The acoustic attenuations of various frequencies are measured at region (2). The lattice attenuation is greatly affected by the rise time of an applied pulse in region (1). It is clear that acoustic flux in the acoustic domain which originates from the amplification of the pure thermally excited acoustic flux attenuates as f^2 and is in accordance with the Akhieser loss. On the other hand, a shock-excited acoustic flux attenuates as $f^{-1.5}$.

PACS numbers: 72.50.+b, 43.35.Qv, 42.80.Ks, 43.35.Sx

There are various reports on the lattice attenuation using the acoustic flux contained in the acoustoelectric domains in CdS,¹⁻³ GaAs,⁴ etc. However, most of the

experimental reports of the frequency dependencies of the lattice attenuations are reported to be proportional to around $f^{1.5}$ and those are different from the expected

Akhieser's f^2 loss.⁵ The authors thought that these deviations from the theoretical value were caused by the domain formation mechanisms. It is supposed that there are two kinds of domain formation mechanisms. One originates from the amplification of the thermally excited acoustic flux around a cathode electrode, and the other originates from the amplification of the shock-excited acoustic flux due to the sudden application of the rapid rise-time high voltage pulse on the insufficient Ohmic contact of the sample.

In this paper, in order to measure the lattice attenuation of the acoustic flux injection method is applied. And it is clear that the acoustic flux in the acoustic domain which originates from the amplification of the pure thermal phonon attenuates as f^2 and is in accordance with the theoretical Akhieser's estimation.

Figure 1 shows the experimental configuration of the acoustic flux injection method⁶ and Brillouin scattering.^{7,8} Experiments were performed by applying an electric field perpendicular to the c axis of the CdS crystal. The typical sample dimensions are shown in Fig. 1. The evaporated indium contacts are made at the middle and both ends of the sample, which divide it into two parts; one part is used as a generation region of the acoustic flux [region (1)] and the other is used as a propagation region of the injected flux [region (2)].

The nonelectronic lattice attenuation can be directly measured in region (2) by applying the electric field (E_{a2}) which produces an electron drift velocity equal to the sound velocity. In order to control the domain formation mechanisms which are the amplification of the thermally excited and/or shock-excited acoustic fluxes, a rise-time variable negative drift pulse was applied on region (1). The applied voltage in region (2), V_2 , is delayed triggered so as to apply just when the acoustic flux is injected into region (2) through the earth electrode. The various characteristics have been studied in region (2) by the Brillouin scattering

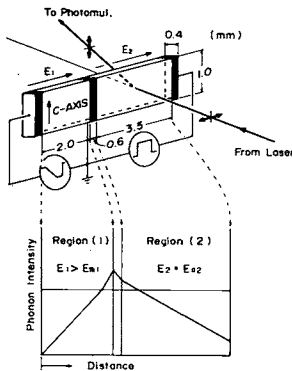


FIG. 1. Configuration of ultrasonic injection method and Brillouin scattering. A rise-time variable voltage pulse is applied on region (1). Lower figure shows the amplification and attenuation of the acoustic flux.

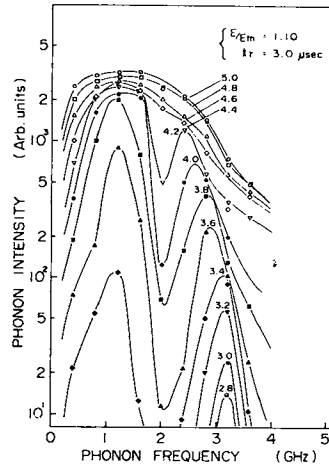


FIG. 2. Phonon spectra of the acoustic flux for $t_r = 3 \mu\text{sec}$. Numerical numbers are distances from the cathode (mm).

method. The deflected light was detected by the photomultiplier, and S/N ratio of the signal was improved by the boxcar integrator and the signal was displayed on an X-Y recorder.

In order to check the effect of the rise time (t_r) of the applied drift pulse in region (1), the phonon spectra of the acoustic flux for a different t_r was observed in the sample which has no earth electrode. Figures 2 and 3 are for $t_r = 3$ and $9 \mu\text{sec}$ of constant applied voltage, respectively. Figures 2 and 3 suggest that the two peaks in Fig. 2 are caused by the shock-excited and the thermally excited acoustic fluxes. By comparing Fig. 2 with Fig. 3, it is supposed that the 3-GHz peak is caused by the thermally excited acoustic flux and the 1-GHz peak is caused by the shock-excited flux. Further, we confirmed that only the 1-GHz peak could be

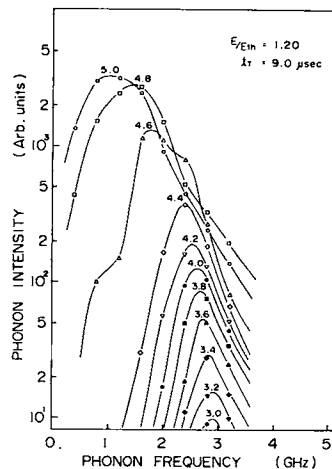


FIG. 3. Phonon spectra of the acoustic flux for $t_r = 9 \mu\text{sec}$.

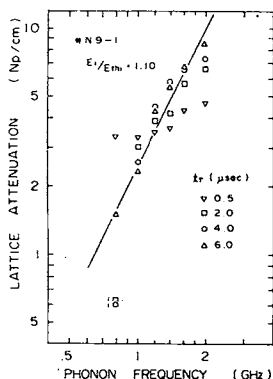


FIG. 4. Frequency dependencies of the lattice attenuation for different t_r . () marked data are not taken into account because these attenuations are due to a different mechanism.

observed for a 0.5-sec rise-time pulse.

Thus we thought that the interactions between these two acoustic fluxes might affect the ultrasonic attenuations. Figure 4 shows the frequency dependencies of the lattice attenuation in region (2) for different t_r in region (1) under the conditions $E_1/E_{th1} = 1.1$ and $E_2 = E_{a2}$.

Here, it is assumed that the lattice attenuation can be represented by $\alpha_1 \propto f^m$. The factor m is measured from Fig. 4 by the method of least-squares fit. The results are shown in Table I together with the correlation coefficients. Table I suggests that for the longer t_r the shock is rejected and the pure thermally excited acoustic flux is amplified and grows up the domain. In this case the factor m approaches 2.

Next, in order to check the effect of the shock excitation, the applied field E_1 is changed when t_r is sustained at 2 μ sec. The application of a 2- μ sec pulse already produces a large amount of shock-excited acoustic wave and the increase in the applied field corresponds to the increase in shock excitation.

Table II shows the results of our experiments. Table II shows that as the applied voltage increases, the factor m approaches 1.5, which is different from 2.

The above experimental results imply that the intensity of the domain does not always determine the value of m , but the origin of the amplified acoustic flux plays an important role in the determination of m . In the usual case these two mechanisms are superimposed and build up to the domain. Therefore, the value of m is different for the ratio of these two components. When

TABLE I. t_r dependencies of m .

Applied field E_1/E_{th1}	1.10			
Rise time (μ sec) t_r	0.5	2.0	4.0	6.0
Slope m	0.53	1.13	1.48	1.99
Correlation coefficient r	0.97	0.97	0.93	0.97

TABLE II. Applied field dependencies of m .

Rise time (μ sec) t_r	2.0			
Applied field E_1/E_{th1}	1.05	1.10	1.20	1.30
Slope m	0.86	1.13	1.46	1.47
Correlation coefficient r	0.33	0.97	0.99	0.99

the thermally excited acoustic flux is dominant (e.g., $t_r = 6 \mu$ sec, $E_1/E_{th1} = 1.1$), the value of m approaches 2. On the other hand, when the shock-excited acoustic flux is dominant, m tends to 1.5; many of the experimental data are between 1.5 and 2. This fact suggests that the two mechanisms are superimposed.

Figure 5 shows the frequency dependencies of the α_1 for the samples in which resistivities are different, $\rho = 4 \Omega \text{ cm}$ and $7 \Omega \text{ cm}$. The electric field and rise times of the applied pulses are fixed and set equal for both samples so as to be $E_1/E_{th1} = 1.1$ and $t_r = 6 \mu$ sec, respectively. In these samples the lattice attenuations are proportional to f^2 and the values are coincident with each other. From the slopes of Fig. 5 α_1/ω^2 can be found to be $6.3 \times 10^{-20} \text{ Np/cm sec}^2$ and $5.3 \times 10^{-20} \text{ Np/cm sec}^2$ for 7 and 4 $\Omega \text{ cm}$, respectively. These values are coincident with the data of Gelbart *et al.*¹ which are obtained from the double-pulse technique to reject the shock excitation.

In conclusion, for the longer t_r , the domain is produced by pure amplification of the thermally excited acoustic flux. In this case, the lattice attenuation is proportional to f^2 for different resistivity samples and the α_1/ω^2 value is around $6 \times 10^{-20} \text{ Np/cm sec}^2$ for both samples.

On the other hand, for a rapid rise-time pulse, the thermally and shock-excited acoustic fluxes interact with each other in a complicated fashion and build up to the acoustic domain. In this domain the lattice attenuation is proportional to f^m and m is sometimes smaller than unity. But when the shock excitation is dominant m tends to 1.5.

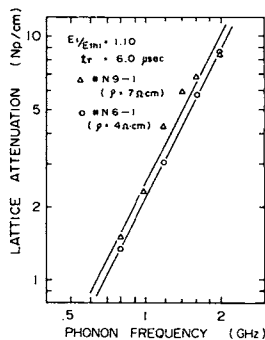


FIG. 5. Frequency dependencies of the lattice attenuation for the sample of different resistivities. Solid line passing through experimental points has the slope of 2.

¹U. Gelbart and A. Many, Phys. Rev. B 7, 2713 (1973).

²M. Yamada, C. Hamaguchi, K. Matsumoto, and J. Nakai, Phys. Rev. B 7, 2673 (1973).

³K. Tsubouchi, S. Kameoka, and T. Arizumi, J. Phys. Soc. Jpn. 37, 1305 (1974).

⁴E.D. Palik and R. Bray, Phys. Rev. B 7, 3302 (1971).

⁵A. Akhiezer, J. Phys. (USSR) 1, 277 (1939).

⁶T. Hata, Y. Tokunaga, and T. Hada, Jpn. J. Appl. Phys. 12, 1956 (1973).

⁷B.W. Hakki and R.W. Dixon, Appl. Phys. Lett. 14, 185 (1969).

⁸C. Hamaguchi, J. Phys. Soc. Jpn. 35, 832 (1973).

⁹T. Hata, T. Nakano, and T. Hada, Proc. 1977 Ultrasonic Symposium, p. 313 (unpublished).